

## NEW DIFFRACTION DATA

# Synthesis and crystal structure refinement of new perovskite oxides, $\text{Dy}_{0.55}\text{Sr}_{0.45}\text{Mn}_{1-x}\text{Fe}_x\text{O}_3$ ( $x = 0.0$ and $0.2$ ) from X-ray powder diffraction data

K. Yadagiri, and R. Nithya<sup>a)</sup>

Materials Science Group, Indira Gandhi Centre for Atomic Research, Kalpakkam 603 102, Tamil Nadu, India

(Received 30 November 2015; accepted 13 June 2016)

Polycrystalline compounds of  $\text{Dy}_{0.55}\text{Sr}_{0.45}\text{Mn}_{1-x}\text{Fe}_x\text{O}_3$  ( $x = 0.0$  and  $0.20$ ) were synthesized using ceramic method and characterized by X-ray powder diffraction technique using  $\text{CuK}\alpha$  ( $1.5406 \text{ \AA}$ ) radiation at room temperature. All the diffraction peaks were indexed to an orthorhombic cell with space group  $Pnma$  (#62). Whole powder diffraction profile refinement was performed using GSAS package. © 2016 International Centre for Diffraction Data. [doi:10.1017/S0885715616000397]

Key words: powder X-ray diffraction, Rietveld refinement, Dy–Sr–Mn–O system

## I. INTRODUCTION

Perovskite manganites have attracted scientific attention since the observation of colossal magneto resistance (CMR) in  $\text{La}_{1-x}\text{A}_x\text{MnO}_3$  ( $A$ , alkaline earth element) in 1990 (review by Dagotto *et al.*, 2001). Cubic perovskites belong to  $Pm\bar{3}m$  space group with one formula unit per unit cell ( $Z = 1$ ) where  $A$  and  $B$  site cations have 12- and sixfold oxygen coordinations (Howard and Stokes, 1998). Crystal structure deviates from the cubic cell depending on the ionic size of cations. Manganates of  $\text{RMnO}_3$  exhibit orthorhombic structure for larger rare earth elements ( $R = \text{La–Dy}$ ) and hexagonal structure for smaller rare earth atoms ( $R = \text{Ho–Lu}$ ). When  $\text{La}$  is replaced by a rare earth ion whose ionic radius is smaller than lanthanum, the coordination of  $A$  site reduces to 8 and 9 depending on the value of the ionic radius.  $\text{REMnO}_3$  belong to multi-functional materials since they exhibit a wide variety of physical properties such as CMR, multi-ferroic behavior, superconductivity, etc. Among the rare earth series,  $\text{DyMnO}_3$  (DMO) exhibits a complex magnetic structure. Low-temperature ground state of  $\text{LaMnO}_3$  is antiferromagnetic (Tokura, 2006), while that of analogous DMO is complex (Goto *et al.*, 2004). There exist two polymorphic structures for DMO depending on the synthesis conditions. High-temperature synthesis (close to its melting point) stabilizes hexagonal structure, whereas synthesis at low temperature results in an orthorhombic phase (Harikrishnan *et al.*, 2008). To induce a stable ferromagnetism into DMO similar to that of  $\text{La}_{1-x}\text{Sr}_x\text{MnO}_3$ , we have chosen Sr and Fe substitutions at Dy and Mn sites in  $\text{Dy}_{0.55}\text{Sr}_{0.45}\text{Mn}_{1-x}\text{Fe}_x\text{O}_3$ . So far, there is no X-ray diffraction (XRD) data of the Dy–Sr–Mn–Fe–O system in the database of ICDD-2014, so we present here our experimental powder XRD data of  $\text{Dy}_{0.55}\text{Sr}_{0.45}\text{MnO}_3$  and  $\text{Dy}_{0.55}\text{Sr}_{0.45}\text{Mn}_{0.8}\text{Fe}_{0.2}\text{O}_3$  to be included in the database.

## II. EXPERIMENTAL

### A. Synthesis

Polycrystalline compounds of  $\text{Dy}_{0.55}\text{Sr}_{0.45}\text{Mn}_{1-x}\text{Fe}_x\text{O}_3$  ( $x = 0.0$  and  $0.2$ ) were prepared by high-temperature

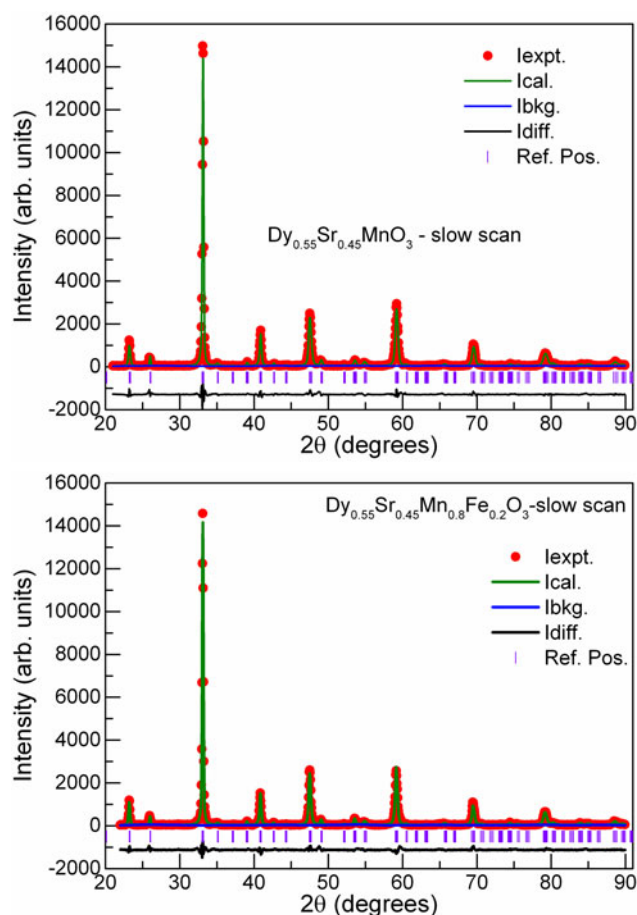


Figure 1. (Color online) Experimental XRD patterns (symbols) for  $\text{Dy}_{0.55}\text{Sr}_{0.45}\text{MnO}_3$  (upper panel) and  $\text{Dy}_{0.55}\text{Sr}_{0.45}\text{Mn}_{0.8}\text{Fe}_{0.2}\text{O}_3$  (lower panel) collected at room temperature. Blue color solid line corresponds to the background intensity ( $I_{\text{bkg.}}$ ). Other solid lines in the figure show calculated intensity (green color –  $I_{\text{calc.}}$ ), difference between experimental and calculated intensities (black –  $I_{\text{diff.}}$ ). The vertical lines shown at the bottom correspond to the expected Bragg reflections for  $Pnma$  space group.

solid-state reaction method, from high-purity oxides (99.99%) of dysprosium oxide ( $\text{Dy}_2\text{O}_3$ ), strontium carbonate ( $\text{SrCO}_3$ ), manganese oxide ( $\text{MnO}_2$ ), and iron oxide ( $\text{Fe}_2\text{O}_3$ ). Starting oxides taken in appropriate ratio to make 2 gm of

<sup>a)</sup> Author to whom correspondence should be addressed. Electronic mail: nithya@igcar.gov.in

TABLE I. Crystallographic data after refinement for  $\text{Dy}_{0.55}\text{Sr}_{0.45}\text{Mn}_{1-x}\text{Fe}_x\text{O}_3$ .

Crystal parameters	$x = 0.00$	$x = 0.20$
Crystal system	Orthorhombic	Orthorhombic
Space group	$Pnma$	$Pnma$
$Z$	4	4
$a$ (Å)	5.4206 (6)	5.4190 (6)
$b$ (Å)	7.6251 (6)	7.6359 (7)
$c$ (Å)	5.4021 (6)	5.4033 (6)
Cell volume (Å <sup>3</sup> )	223.285 (13)	223.585 (13)
$R$ -factors		
$\chi^2$	3.886	4.153
$R$ ( $F^2$ )	3.56	4.26
$R_p$	9.94	10.53
$wR_p$	14.23	15.56

the final compounds were ground with the help of an agate mortar and pestle for several hours in order to get a homogeneous mixture. Mixed powders were calcined in air at 1573 K for 10 h with intermediate grinding until the formation of single-phase compounds.

### B. XRD data acquisition

Powder XRD patterns of the compounds were collected at room temperature using STOE (Germany) X-ray powder

diffractometer operated in Bragg–Brentano parafocusing geometry with fixed slits. The diffraction data were collected at room temperature with a scintillation detector, NaI (TI) using  $\text{CuK}\alpha$  radiation (1.5406 Å) operated at 40 kV and 30 mA. The diffractometer is equipped with a secondary monochromator, which is flat pyrolytic graphite. The angular range of the scan was from 21° to 90° with a step size of 0.05° and a count time per step was 30–40 s. The powder was loaded in a (911) Si single-crystal wafer holder, which gives a zero background intensity in the  $2\theta$  measurement range studied.

### III. RESULTS

Observed XRD patterns (solid symbols) of  $\text{Dy}_{0.55}\text{Sr}_{0.45}\text{MnO}_3$  (upper panel) and  $\text{Dy}_{0.55}\text{Sr}_{0.45}\text{Mn}_{0.8}\text{Fe}_{0.2}\text{O}_3$  (lower panel) are shown in Figure 1. Rietveld structure refinement of the whole powder XRD data using EXPGUI version (Larson and Von Dreele, 2000) of GSAS program was undertaken. Background intensity was well fitted by a linear interpolation function. Among the four functions available in GSAS to represent the diffraction profiles, Pseudo-Voigt function (type II), which is the weighted sum of a Gaussian and Lorentzian functions was used during the refinement. All the diffraction peaks were adequately represented by this function where all the profile parameters were refined. While refining the

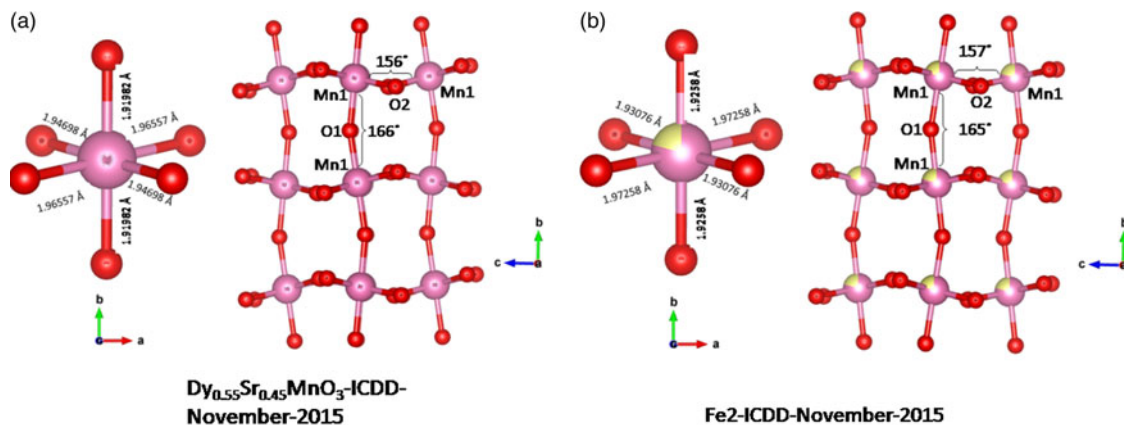


Figure 2. (Color online) Schematic diagram of octahedral arrangement of Mn–O chains along the  $b$ -axis in (a) DSMO and (b) DSMFO, pink/yellow spheres correspond to Mn/Fe ions and oxygen ions are shown by red spheres. Deviations in the bond angles (Mn–O–Mn) and bond distances (Mn–O) from the ideal cubic perovskite structure are seen. Bond distances (Mn–O) in the  $\text{MnO}_6$  and bond angles in the plane (Mn1–O2–Mn1) and along the  $b$ -axis (Mn1–O1–Mn1) are marked in the figure.

TABLE II. Fractional coordinates obtained from Rietveld refinement of  $\text{Dy}_{0.55}\text{Sr}_{0.45}\text{Mn}_{1-x}\text{Fe}_x\text{O}_3$  for  $x = 0.0$  and  $0.2$ .

Atom label	Atom type	Wyckoff site	$x$	$y$	$z$	Occupancy
$x = 0.0$						
Dy1/Sr1	$\text{Dy}^{+3}/\text{Sr}^{+2}$	4	0.030 120 ± 0.000 482	0.25	0.998 048 ± 0.003 419	0.55/0.45
Mn1	$\text{Mn}^{+3}$	4	0	0	0.5	1.0
O1	$\text{O}^{-2}$	4	0.501 399	0.25	0.042 098	1.0
O2	$\text{O}^{-2}$	8	0.220 586	0.545 405	0.222 876	1.0
$x = 0.2$						
Dy1/Sr1	$\text{Dy}^{+3}/\text{Sr}^{+2}$	4	0.029 129 ± 0.000 375	0.25	0.997 149 ± 0.001 605	0.55/0.45
Mn1/Fe1	$\text{Mn}^{+3}/\text{Fe}^{+3}$	4	0	0	0.5	0.8/0.2
O1	$\text{O}^{-2}$	4	0.500 907	0.25	0.046 997	1.0
O2	$\text{O}^{-2}$	8	0.219 771	0.542 345	0.225 186	1.0

TABLE III. Selected inter-atomic distances (Å) and bond angle (°) for Dy<sub>0.55</sub>Sr<sub>0.45</sub>Mn<sub>1-x</sub>Fe<sub>x</sub>O<sub>3</sub> obtained from the Rietveld refinement structure model used to refine whole powder diffraction patterns.

Atom	$x = 0.00$	Atom	$x = 0.20$
Mn–O octahedron		Mn/Fe–O octahedron	
Mn1–O1	1.919 82 (15) × 2	Mn1/Fe1–O1	1.925 80 (27) × 2
Mn1–O2	1.965 57 (16) × 2	Mn1/Fe1–O2	1.972 58 (19) × 2
	1.946 98 (16) × 2		1.930 76 (18) × 2
O1–Mn1–O1	180.00 (0)	O1–Mn1/Fe1–O1	180.00 (0)
O1–Mn1–O2	96.049 (2) × 2	O1–Mn1/Fe1–O2	94.768 (3) × 2
	85.235 (2) × 2	O1–Mn1/Fe1–O2	86.387 (3) × 2
	83.951 (2) × 2	O1–Mn1/Fe1–O2	85.232 (3) × 2
	94.765 (2) × 2	O1–Mn1/Fe1–O2	93.613 (3) × 2
O2–Mn1–O2	180.00 (0)	O2–Mn1/Fe1–O2	180.00 (0)
	88.334 (9) × 2		88.453 (10) × 2
	91.666 (9) × 2		91.547 (10) × 2
Mn1–O1–Mn1	166.386 (2)	Mn1/Fe1–O1–Mn1/Fe1	164.843 (3)
Mn1–O2–Mn1	155.908 (2)	Mn1/Fe1–O2–Mn1/Fe1	157.190 (3)

fractional coordinates of cations, Dy, Sr and Mn, Fe ions, their  $x$ ,  $y$ , and  $z$  parameters were constrained. Isotropic thermal parameters were chosen during the refinement. All the diffraction peaks were indexed using orthorhombic structure with space group  $Pnma$ . XRD patterns thus calculated matched satisfactorily with the experimental patterns and are included along with the observed patterns in Figure 1.

Crystal data after the final refinement are presented in Table I. Corresponding set of  $R$  parameters, which indicate the quality of the fit are also included in Table I.

Fe substitution in the parent compound did not bring noticeable changes in lattice parameters. Figure 2 depicts ball-and-stick representation of crystal structure using Visualization for Electronic and Structural Analysis (Vesta) software (Momma and Izumi, 2013) of the unit cell where corner sharing Mn–O octahedra are arranged along the  $b$ -axis for both compounds. A single MnO<sub>6</sub> along with bond distances is displayed in the same figure. It is apparent from the figure that there are significant distortions in bond distances and bond angles by nearly partial substitution of Sr at the Dy site.

Fractional coordinates used for the refinement for both compounds are tabulated in Table II. Selected bond lengths and bond angles are given in Table III together with their estimated standard deviations. Each Mn atom is coordinated by six oxygen atoms with three pairs of different bond distances. The apical bond lengths (Mn–O1) are shorter than the in-plane

Mn–O2 bond lengths. Our refinement results also indicate that Dy is ninefold coordinated with oxygen ions and the bond lengths of Dy–O vary between 2.4 and 2.9 Å.

## SUPPLEMENTARY MATERIAL

The supplementary material for this article can be found at <http://dx.doi.org/10.1017/S0885715616000397>.

- Dagotto, E., Hotta, T., and Moreo, A. (2001). “Colossal magnetoresistant materials: the key role of phase separation,” *Phys. Rep.* **344**, 1–153.
- Goto, T., Kimura, T., Lawes, G., Ramirez, A. P., and Tokura, Y. (2004). “Ferroelectricity and giant magnetocapacitance in perovskite rare-earth manganites,” *Phys. Rev. Lett.* **92**, 257201.
- Harikrishnan, S., Naveen Kumar, C. M., Bhat, H. L., Elizabeth, S., Robler, U. K., Dorr, K., Robler, S., and Wirth, S. (2008). “Investigations on the spin-glass state in Dy<sub>0.5</sub>Sr<sub>0.5</sub>MnO<sub>3</sub> single crystals through structural, magnetic and thermal properties,” *J. Phys.: Condens. Matter.* **20**, 275234.
- Howard, C. J. and Stokes, H. T. (1998). “Group-theoretical analysis of octahedral tilting in perovskites,” *Acta Crystallogr. B* **54**, 782–789.
- Larson, A. C. and Von Dreele, R. B. (2000). *General Structure Analysis System (GSAS)* (Los Alamos National Laboratory Report LAUR 86-748).
- Momma, K. and Izumi, F. (2013). “VESTA 3 for three-dimensional visualization of crystal, volumetric and morphology data,” *J. Appl. Crystallogr.* **44**, 1272–1276.
- Tokura, Y. (2006). “Critical features of colossal magneto resistive manganites,” *Rep. Prog. Phys.* **69**, 797.